Received: 23 January 2024 | Accepted: 5 April 2024

DOI: 10.1097/HC9.0000000000000483

ORIGINAL ARTICLE

OPEN

Retinoic acid generates a beneficial microenvironment for liver progenitor cell activation in acute liver failure

Sai Wang[1] | Frederik Link[1] | Stefan Munker[2,3] | Wenjing Wang[4] | Rilu Feng[1,5] | Roman Liebe[6] | Yujia Li[1] | Ye Yao[1] | Hui Liu[7] | Chen Shao[7] | Matthias P.A. Ebert[1,8,9] | Huiguo Ding[10] | Steven Dooley[1] | Hong-Lei Weng[1] | Shan-Shan Wang[4]

[1]Department of Medicine II, University Medical Center Mannheim, Medical Faculty Mannheim, Heidelberg University, Mannheim, Germany

[2]Department of Medicine II, University Hospital, LMU Munich, Munich, Germany

[3]Liver Center Munich, University Hospital, LMU, Munich, Germany

[4]Beijing Institute of Hepatology, Beijing You'an Hospital, Capital Medical University, Beijing, China

[5]Department of Endocrinology and Metabolism, Renji Hospital, School of Medicine, Shanghai Jiao Tong University, Shanghai, China

[6]Clinic of Gastroenterology, Hepatology and Infectious Diseases, Otto-von-Guericke-University, Magdeburg, Germany

[7]Department of Pathology, Beijing You'an Hospital, Affiliated with Capital Medical University, Beijing, China

[8]Molecular Medicine Partnership Unit, European Molecular Biology Laboratory, Heidelberg, Germany

[9]DKFZ-Hector Cancer Institute at the University Medical Center, Mannheim, Germany

[10]Department of Gastroenterology and Hepatology, Beijing You'an Hospital, Affiliated with Capital Medical University, Beijing, China

Correspondence
Shan-Shan Wang, Beijing Institute of Hepatology, Beijing You'an Hospital, Capital Medical University, No. 8 Xi Tou Tiao, You An Men Wai, Feng Tai District, Beijing 100069, China.
Email: wangshanshan1987@ccmu.edu.cn

Abstract

Background: When massive necrosis occurs in acute liver failure (ALF), rapid expansion of HSCs called liver progenitor cells (LPCs) in a process called ductular reaction is required for survival. The underlying mechanisms governing this process are not entirely known to date. In ALF, high levels of retinoic acid (RA), a molecule known for its pleiotropic roles in embryonic development, are secreted by activated HSCs. We hypothesized that RA plays a key role in ductular reaction during ALF.

Methods: RNAseq was performed to identify molecular signaling pathways affected by all-*trans* retinoid acid (atRA) treatment in HepaRG LPCs. Functional assays were performed in HepaRG cells treated with atRA or cocultured with LX-2 cells and in the liver tissue of patients suffering from ALF.

Abbreviations: ABC, ATP-binding cassette; ACAA1, acetyl-CoA acyltransferase 1; ACSL5, acyl-CoA synthetase long chain family member 5; AFP, alpha fetoprotein; ALF, acute liver failure; APOA1, apolipoprotein A1; atRA, all-*trans* retinoid acid; CEBP, CCAAT enhancer binding protein; CLTR, China Liver Transplant Registry; COL1A1, collagen, type I, alpha 1; CPT1B, palmitoyltransferase 1B; FBS, fetal bovine serum; GATA6, GATA binding protein 6; IF, immunofluorescence; LPC, liver progenitor cell; LPL, lipoprotein lipase; MMP2/9, matrix metalloproteinase 2/9; phHSC, primary human hepatic stellate cell; PLIN1/5, perilipin 1/5; POLK, DNA polymerase kappa; P/S, penicillin/streptomycin; RA, retinoic acid; RAR, retinoic acid receptor; RXR, retinoid X receptor; SOX9, SRY-box transcription factor 9; α-SMA, alpha-smooth muscle actin.

Sai Wang and Frederik Link contributed equally to this work.

Supplemental Digital Content is available for this article. Direct URL citations are provided in the HTML and PDF versions of this article on the journal's website, www.hepcommjournal.com.

Results: Under ALF conditions, activated HSCs secreted RA, inducing RARα nuclear translocation in LPCs. RNAseq data and investigations in HepaRG cells revealed that atRA treatment activated the WNT-β-Catenin pathway, enhanced stemness genes (SOX9, AFP, and others), increased energy storage, and elevated the expression of ATP-binding cassette transporters in a RARα nuclear translocation-dependent manner. Further, atRA treatment–induced pathways were confirmed in a coculture system of HepaRG with LX-2 cells. Patients suffering from ALF who displayed RARα nuclear translocation in the LPCs had significantly better MELD scores than those without.

Conclusions: During ALF, RA secreted by activated HSCs promotes LPC activation, a prerequisite for subsequent LPC-mediated liver regeneration.

INTRODUCTION

Massive hepatic necrosis occurs during the final and frequently lethal stages of acute liver failure (ALF) when only a few intact hepatocytes remain.[1] Hepatocytes perform the majority of hepatic functions, for example, the production of bile acids and various plasma proteins, including coagulation factors, nutrient storage and metabolism, elimination of xenobiotics, steroid hormones, and cytokines to support systemic homeostasis.[2] Intriguingly, some patients with ALF in whom most of the hepatocytes are damaged can recover following acute decompensation. The underlying mechanisms are thought to be dependent on liver progenitor cells (LPCs).[3,4] LPCs are stem-like cells that reside along the canals of Hering and biliary ductules of healthy livers. They proliferate rapidly in severely damaged livers and can be identified by immunohistochemical staining for biliary markers, such as CK19 and CK7.[1,5] The mechanisms that regulate LPC activation, most likely through signals from the surrounding microenvironment, remain largely unknown.

HSCs constitute 5%–8% of all liver cells[6] and contain ~80% of the body's vitamin A (retinol). Retinol is metabolized into retinoic acid (RA) in 2 steps and has pleiotropic functions in embryonic development[7] and liver homeostasis.[8] In vivo, during liver injury or in vitro, during cell culture, HSCs are activated, secrete retinoids rapidly, and upregulate their production of profibrogenic cytokines (eg, TGF-β1) and extracellular matrix components.[9,10] The retinoids liberated from lipid droplets during HSC activation can be used for RA formation, whose biological effects are mainly mediated through 2 nuclear receptors: retinoic acid receptor (RAR) and retinoid X receptor (RXR).[11,12] all-*trans* retinoid acid (atRA) is believed to be the endogenous ligand for RAR at nanomolar levels, especially RARα, the most abundant isoform in the liver.[13] According to studies, atRA-RAR/RXR pathways promote fatty acid oxidation while inhibiting lipid and bile acid synthesis in hepatocytes.[14,15] atRA also demonstrates inhibitory effects on the expression of profibrotic genes, including TGF-β1, collagen type 1, alpha 1 (COL1A1), MMP2, and α-SMA in HSCs through RAR-dependent downregulation of myosin light chain 2 expression on a transcriptional level.[16–18] In addition, RA has been shown to reduce hepatic inflammation by repressing the production of proinflammatory cytokines in dendritic cells, monocytes, macrophages, and T cells in an RAR/RXR-dependent manner,[19–21] thereby regulating immune cell differentiation and activation.[19,22] Devalaraja et al[23] found that tumor-derived RA polarizes intratumoral monocyte differentiation toward tumor-associated macrophages and away from immunostimulatory dendritic cells, thus promoting immune suppression. Furthermore, the inhibition of RA signaling within tumor microenvironment enhances T-cell–dependent antitumor immunity, providing a potential target for tumor immunotherapy.[23] The findings of Gundra et al[24] emphasize the essential role of RA in the transformation of monocyte-derived macrophages into tissue-resident macrophages. Considering that circulating monocytes have the capacity to give rise to liver-resident Kupffer cells,[25] RA likely plays a crucial role in this process as well. Under ALF conditions, with high levels of RA secreted by activated HSCs, the effects of RA on LPCs remain inadequately understood.

In this study, we investigated the effects of RA on the HepaRG LPC line using RNA sequencing (RNAseq) in vitro and further verified our findings in vivo using liver tissue from patients with ALF.

METHODS

Reagents and antibodies

atRA (cat. #R2625-100MG, Sigma-Aldrich); Human RARα siRNA (cat. #sc-29465, Santa Cruz Biotechnology); RARα antibody (cat. #PA5-39870, Cell Signaling Technology);

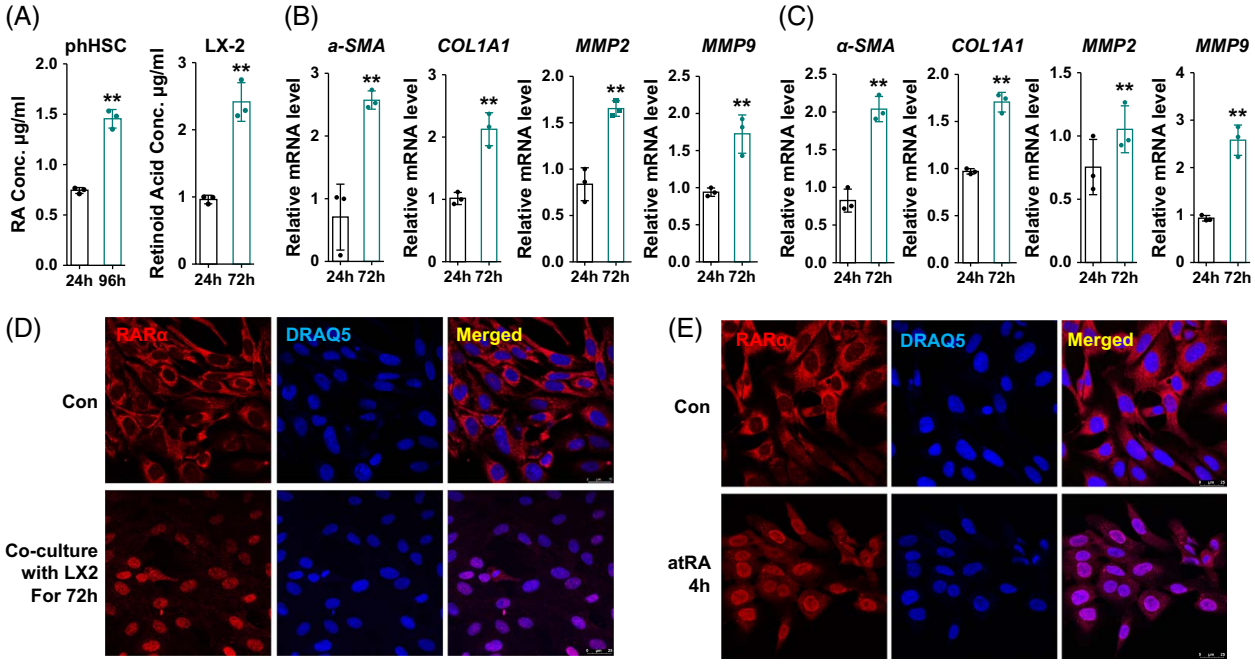

FIGURE 1 RA activates RARα signaling in HepaRG cells. (A) The concentration of retinoic acid (µg/mL) secreted by phHSCs or LX-2 cells by absorbance measurement at 352 nm. (B, C) Relative mRNA levels of α-SMA, COL1A1, MMP2, and MMP9 were determined by qrtPCR in phHSCs and LX-2 cultured for 96 or 72 hours respectively. (D, E) Expression and location of RARα were detected by immunofluorescence staining in HepaRG cells cocultured with/without LX-2 cells for 72 hours or treated with/without atRA for 4 hours. For qrtPCR, human PPIA was used as the endogenous control. Bars represent mean ± SD. $^{**}p < 0.01$. For IF, DRAQ5 was used to stain the nuclei. Scale bars, 25 µm. Images were chosen representatively from 3 independent experiments. Abbreviations: atRA, all-*trans* retinoid acid; IF, immunofluorescence; phHSC, primary human hepatic stellate cells; RA, retinoic acid.

Active β-Catenin antibody (cat. #05-665, Millipore); β-Catenin antibody (cat. #sc-7963, Santa Cruz Biotechnology); SOX9 antibody (cat. #82630, Cell Signaling Technology); AFP antibody (cat. #HPA010607, Sigma-Aldrich); MRP1 antibody (cat. #sc-18835, Santa Cruz Biotechnology); Alexa Fluor 555 goat anti-mouse IgG (cat. #A-21422, Invitrogen); Alexa Flour 488 goat anti-rabbit IgG (cat. #A-11008, Invitrogen); DRAQ5 (cat. #4084L, Cell Signaling Technology); GAPDH antibody (cat. #32233, Santa Cruz Biotechnology); Histone H1 antibody (cat. #8030, Santa Cruz Biotechnology); BODIPY (D-3922, Life Technologies); Insulin-Transferrin-Selenium (ITS-G) (100X) (cat. #41400045, Thermo Fisher Scientific).

Liver tissue specimens of patients

Twenty-one liver tissue samples of patients with ALF were collected at the Beijing You'an Hospital, Affiliated with Capital Medical University and at the Department of Medicine II, University Medical Centre Mannheim, Medical Faculty Mannheim, Heidelberg University. In this study, ALF was defined as an acute decompensation occurring in individuals regardless of the presence of prior liver damage. Acute decompensation was diagnosed as: (i) total bilirubin >10 upper limit of normal or increased total bilirubin 1 mg/d with or without grade 2 to 3 ascites within <2 weeks; (ii) overt HE; (iii) gastrointestinal hemorrhage; (iv) international normalized ratio ≥ 1.5, (v) bacterial infections (spontaneous bacterial peritonitis, spontaneous bacteremia, urinary tract infection, pneumonia, and cellulitis).[26] The liver tissue from 21 patients with ALF was collected when they underwent liver transplantation. The study protocol was approved by the local ethics committees (Jing-2015-084 and 2017-584N-MA). Written informed consent was obtained from patients or their representatives. Organ allocation and timing of liver transplantation were governed by the China Liver Transplant Registry (CLTR),[27] an official organization for scientific registry authorized by the Chinese Health Ministry, according to the MELD score of the patient.

Primary human stellate cell isolation

Primary human hepatic stellate cells (phHSCs) were isolated at the Cell Isolation Core Facility of the Biobank Großhadern, University Hospital, LMU Munich, using discontinuous density centrifugation with percoll.[28] phHSCs were grown in 10% DMEM supplemented with 1% L-glutamine, 1% penicillin/streptomycin (P/S), and 10% fetal bovine serum (FBS). All cells were kept in a humidified 37°C incubator enriched with 5% CO_2.

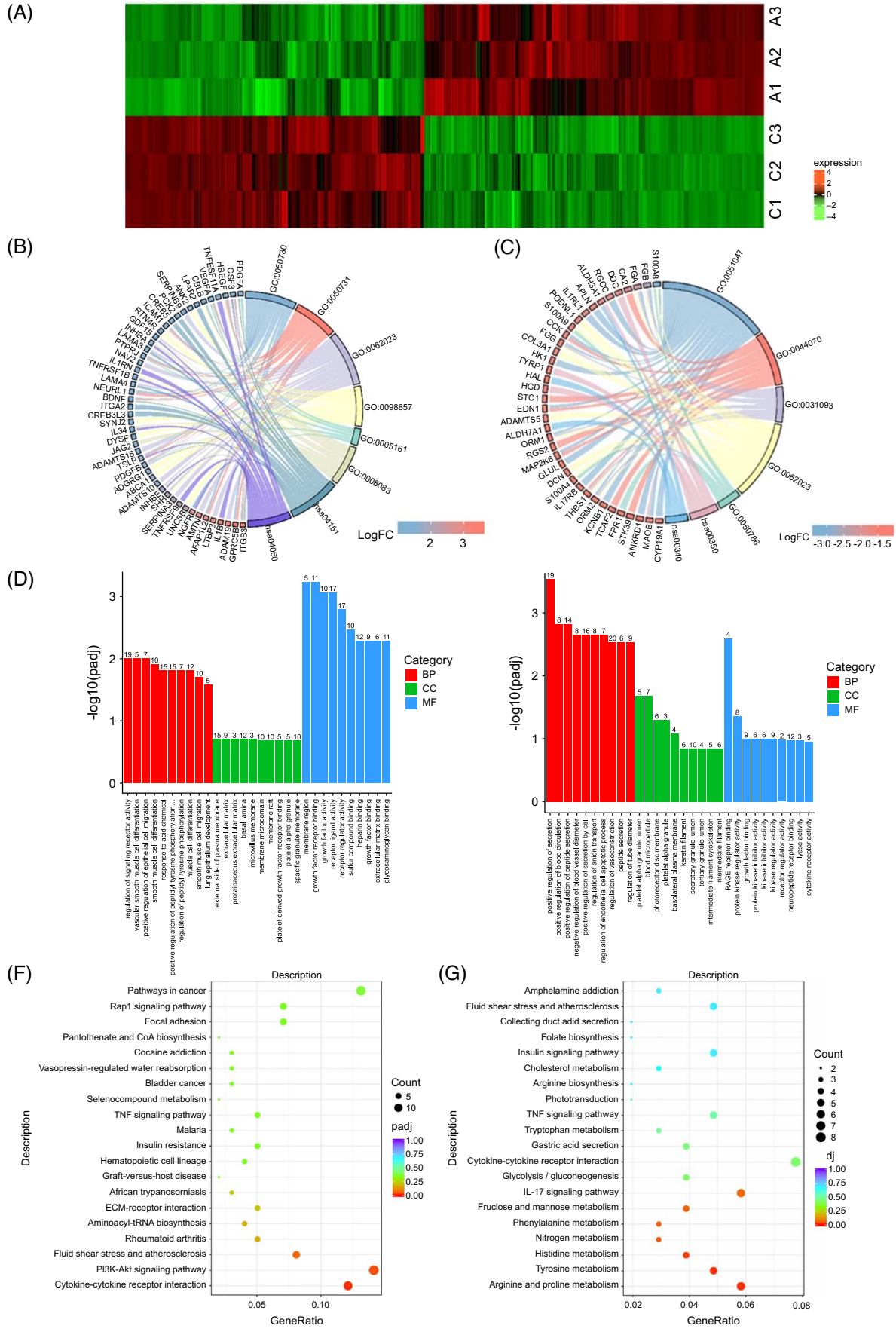
(A)
A3
A2
A1
C3
C2
C1
expression
4
2
0
−2
−4
(B)
GO:0050730
GO:0050731
GO:0062023
GO:0098857
GO:0005161
GO:0008083
hsa04151
hsa04060
LogFC
2
3
(C)
GO:0051047
GO:0044070
GO:0031093
GO:0062023
GO:0050786
hsa00350
hsa00340
LogFC
-3.0 -2.5 -2.0 -1.5
(D)
-log10(padj)
Category
BP
CC
MF
(F)
Description
Pathways in cancer
Rap1 signaling pathway
Focal adhesion
Pantothenate and CoA biosynthesis
Cocaine addiction
Vasopressin-regulated water reabsorption
Bladder cancer
Selenocompound metabolism
TNF signaling pathway
Malaria
Insulin resistance
Hematopoietic cell lineage
Graft-versus-host disease
African trypanosomiasis
ECM-receptor interaction
Aminoacyl-tRNA biosynthesis
Rheumatoid arthritis
Fluid shear stress and atherosclerosis
PI3K-Akt signaling pathway
Cytokine-cytokine receptor interaction
GeneRatio
Count
padj
(G)
Description
Amphetamine addiction
Fluid shear stress and atherosclerosis
Collecting duct acid secretion
Folate biosynthesis
Insulin signaling pathway
Cholesterol metabolism
Arginine biosynthesis
Phototransduction
TNF signaling pathway
Tryptophan metabolism
Gastric acid secretion
Cytokine-cytokine receptor interaction
Glycolysis / gluconeogenesis
IL-17 signaling pathway
Fructose and mannose metabolism
Phenylalanine metabolism
Nitrogen metabolism
Histidine metabolism
Tyrosine metabolism
Arginine and proline metabolism
GeneRatio
Count
dj

FIGURE 2 RNAseq analysis of HepaRG cells treated with control or atRA. (A) Heatmap of the upregulated and downregulated genes in response to atRA treatment in HepaRG cells. (B, C) Chord diagram, illustrating the main biological processes the downregulated or upregulated genes are involved in. (D, E) Enrichment score analysis of control versus atRA treatment. (F, G) GO enrichment analysis of control versus atRA treatment. Abbreviations: atRA, all-*trans* retinoid acid; GO, gene ontology; RNAseq, RNA sequencing.

Cell culture and treatment

The HepaRG cell line is a human bipotent LPC line.[29] HepaRG cells were kept in William's E medium supplemented with 10% FBS, 1% L-glutamine, 1% P/S, 50 μM hydrocortisone hemisuccinate, and 5 μg/mL insulin. LX-2 HSCs were kept in DMEM supplemented with 2% FBS, 1% L-glutamine, and 1% P/S. Following overnight culture, HepaRG cells were transfected with control or RARα siRNA, treated with control or 10 μM atRA for 24 hours, or cocultured with LX-2 HSCs in trans-well for 72 hours before the sample collection for further analysis. To induce HepaRG differentiation to hepatocyte, the cells were cultured in differentiation medium (William's E medium supplemented with 10% FBS, 1% L-glutamine, 1% P/S, 1× Insulin-Transferrin-Selenium [ITS-G] [100×], 50 ng/mL EGF, 40 ng/mL dexamethasone, and 10 mM nicotinamide) for 2, 4, or 7 days.

MTT assay

Proliferation measurements were performed using the thiazolyl blue tetrazolium bromide (MTT) assay. Four thousand cells per well were seeded in quadruplicate in a 96-well plate. After attachment, cells were treated as described in the Cell culture and treatment section. At the end of all other experiments, the remaining cell culture medium was discarded, and 100 μL of fresh culture medium and 10 μL MTT reagent were added to each well and incubated for 4 hours at 37°C to enable the formation of formazan crystals. Next, the medium was discarded, and 100 μL/well of DMSO was added. The plate was incubated on a shaker at room temperature for 10 minutes to dissolve the formazan crystals. Absorbance was measured at 570 nm using the Tecan Infinite M200 Spectrophotometer.

Western blotting

For whole-cell lysates, cultured cells were washed with ice-cold PBS and dissolved in RIPA lysis buffer (1% Triton X-100, 50 mMTris [pH 7.5], 300 mM NaCl, 1 mM ethylene glycol-bis (β-aminoethyl ether)- N,N,N′, N′-tetraacetic acid, 1 mM EDTA, and 0.1% sodium dodecyl sulfate), with freshly added phosphatase and protease inhibitors. Protein concentrations were measured using the Bio-Rad protein assay kit according to the manufacturer's instructions and were quantified using the Tecan Infinite M200 through absorbance measurement at 690 nm. Twenty micrograms of protein were separated by sodium dodecyl sulfate-PAGE (10%–12% gels) and blotted onto a nitrocellulose membrane (Millipore). The membrane was blocked with 5% bovine serum albumin in tris buffered saline with Tween-20 at room temperature for 1 hour. Subsequently, the membrane was incubated with primary antibodies overnight at 4°C. The following day, the membrane was incubated with horseradish peroxidase-linked anti-mouse or anti-rabbit secondary antibody. Signals were visualized by the Supersignal Ultra solution (Pierce) and recorded by the imaging system Fusion SL4 (PEQLAB). For liver tissue, 20 μg of extracted proteins were used for western blotting. Each western blotting experiment was repeated at least 3 times.

Nuclear and cytosolic extracts

Nuclear and cytoplasmic extracts were performed as described.[30] Briefly, HepaRG cells were collected in subcellular fractionation buffer with 250 mM sucrose, 20 mM HEPES (pH 7.4), 10 mM potassium chloride, 1.5 mM $MgCl_2$, 1 mM EDTA, 1 mM ethylene glycol-bis (β-aminoethyl ether)- N,N,N′,N′-tetraacetic acid, 1 mM dithiothreitol, and phosphatase inhibitor cocktail 2. Following agitation at 30–50 rpm on a tube roller at 4°C for 30 minutes, the cells were centrifuged at 720*g*, 4°C for 5 minutes. The supernatant was transferred to a new tube and was centrifuged at 1000*g*, 4°C for 10 minutes to obtain the cytosolic fraction. Subsequently, the pellet was washed by a subcellular fractionation buffer and was centrifuged at 720*g*, 4°C for 10 minutes. The pellet was resuspended in nuclear lysis buffer and agitated at 4°C for 15 minutes to obtain the nuclear fraction.

Transfection and RNA interference

For gene silencing experiments, cells were transfected by 50 nM siRNA using Lipofectamine RNAiMAX (Invitrogen) following the manufacturer's protocol. Cells were harvested 48 hours after transfection.

RNA isolation and qRT-PCR

RNA was isolated from liver tissues or cultured cells with the TRIZOL reagent (Sigma-Aldrich). 500 ng RNA was

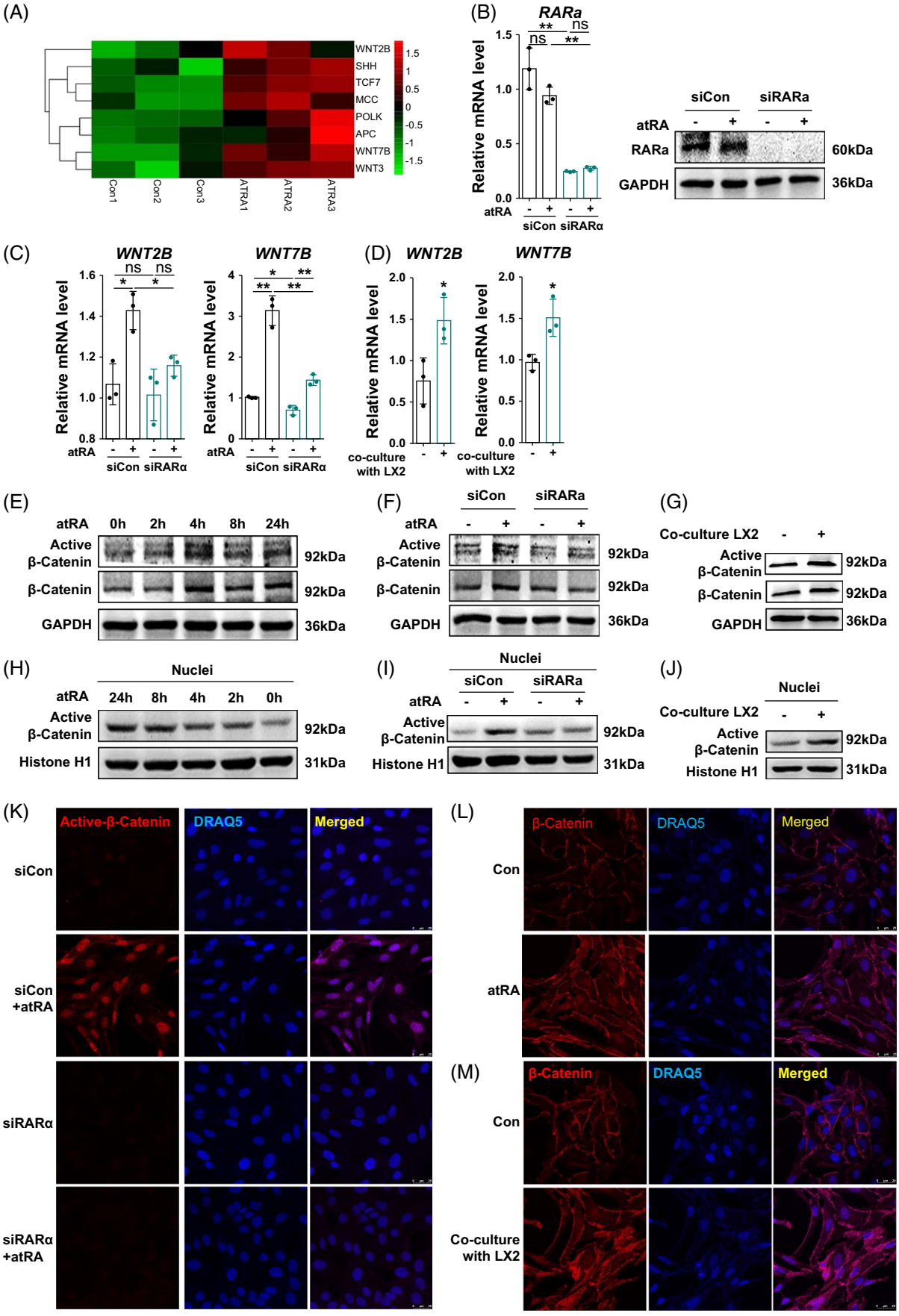
(A)
WNT2B
SHH
TCF7
MCC
POLK
APC
WNT7B
WNT3
1.5
1
0.5
0
-0.5
-1
-1.5
Con1
Con2
Con3
ATRA1
ATRA2
ATRA3
(B)
RARa
Relative mRNA level
ns
**
atRA
siCon siRARα
siCon
siRARa
RARa
GAPDH
60kDa
36kDa
(C)
WNT2B
WNT7B
Relative mRNA level
atRA
siCon siRARα
(D)
WNT2B
WNT7B
Relative mRNA level
co-culture with LX2
(E)
atRA 0h 2h 4h 8h 24h
Active β-Catenin
β-Catenin
GAPDH
92kDa
36kDa
(F)
siCon siRARa
atRA
(G)
Co-culture LX2
(H)
Nuclei
atRA 24h 8h 4h 2h 0h
Histone H1
31kDa
(I)
(J)
(K)
Active-β-Catenin
DRAQ5
Merged
siCon
siCon +atRA
siRARα
siRARα +atRA
(L)
β-Catenin
Con
atRA
(M)
Co-culture with LX2

FIGURE 3 RA activates WNT signaling in HepaRG cells. (A) Heatmap showing the upregulated genes in the WNT pathway. (B) Relative mRNA level and protein expression of RARα in HepaRG cells treated with/without atRA followed by transfection of control or RARα siRNA. (C) Relative mRNA levels of WNT2B and WNT 7B in HepaRG cells treated with/without atRA followed by transfection of control or RARα siRNA. (D) Relative mRNA levels of WNT2B and WNT 7B in HepaRG cells cocultured with/without LX-2 cells for 72 hours. (E) Protein levels of active β-Catenin and total β-Catenin were determined by western blotting in HepaRG cells treated with atRA for 0, 2, 4, 8, 24 hours. (F) Protein levels of active β-Catenin and total β-Catenin were determined by western blotting in HepaRG cells treated with/without atRA followed by transfection of control or RARα siRNA. (G) Protein levels of active β-Catenin and total β-Catenin were determined by western blotting in HepaRG cells cocultured with/without LX-2 cells for 72 hours. (H–J) Nuclear protein level of active β-Catenin in HepaRG cells with the treatment as shown in the figures. (K) Location of active β-Catenin was detected by immunofluorescence staining in HepaRG cells treated with/without atRA followed by transfection of control or RARα siRNA. (L, M) Location of total β-Catenin was detected by immunofluorescence staining in HepaRG cells treated with/without atRA for 24 hours or cocultured with/without LX-2 for 72 hours. For qrtPCR, human PPIA was used as the endogenous control. Bars represent mean ± SD. $^{*}p < 0.05$; $^{**}p < 0.01$. For western blotting, GAPDH was used as the loading control. Histone H1 was used as the loading control of nuclear protein. For IF, DRAQ5 was used to stain the nuclei. Scale bars, 25 μm. Images were chosen representatively from 3 independent experiments. Abbreviations: atRA, all-*trans* retinoid acid; IF, immunofluorescence; RA, retinoic acid.

used for cDNA synthesis with a cDNA synthesis kit (Thermo Fisher). A 20 μL mixture containing 5 μL cDNA (diluted 1:10), 4 μL SYBR Green, and 10 μM of both forward and reverse primers was used for real-time PCR in a StepOnePlus Real-Time PCR instrument (Applied Biosystems). Amplification for qRT-PCR comprised a polymerase activation step for 10 minutes at 95°C, a subsequent amplification for 15 seconds at 95°C and 1 minute at 60°C in 40 cycles. A melting curve was detected to validate the specificity of each PCR analysis. Results were normalized against the housekeeping gene PPIA. Primer sequences were retrieved from the PrimerBank (Massachusetts General Hospital) online resource and ordered from Eurofins Genomics (Eurofins Scientific) (Supplemental Table S1, http://links.lww.com/HC9/A950).

Chromatin immunoprecipitation

Chromatin immunoprecipitation was performed according to a previous description.[31] 1×10^6 HepaRG cells treated with control or atRA for 24 hours were collected and prepared for ChIP assay. Two micrograms of RARα antibody or rabbit IgG were used for incubation with the samples. The control or RARα antibody-pulled down DNA was extracted and used for PCR analysis. Primer sequences of *CTNBB1* and *SRY-box transcription factor 9 (SOX9)* for ChIP assay are shown in Supplemental Table S1, http://links.lww.com/HC9/A950.

Immunofluorescence staining

Cultured cells were fixed on slides with 4% paraformaldehyde for 10 minutes. After washing with PBS for 3 times, slides were permeabilized with 0.5% Triton X-100 in PBS for 10 minutes. After rinsing the samples with PBS, cells were blocked with 0.025% Triton X-100 and 1% bovine serum albumin in PBS for 1 hour at room temperature. Subsequently, the slides were incubated with primary antibodies in PBS, 0.025% Triton X-100, and 1% bovine serum albumin at 4°C overnight. The next day, all slides were incubated with fluorochrome-conjugated secondary antibodies and DRAQ5 (Invitrogen) for 1 hour followed by 3 washes with PBS plus 0.025% Triton X-100. Images were recorded with a Leica Confocal TCS SPE microscope.

Immunohistochemistry staining

Liver sections of 4 μm thickness were used for immunohistochemistry staining. After deparaffinization, sections were washed in PBS for 3 times. Heat-induced antigen retrieval was performed in EDTA buffer, and endogenous peroxidase activity was blocked by Dako blocking reagent. The slides were incubated with primary antibody or PBS (negative control) overnight at 4°C. The following day, the slides were incubated with streptavidin-conjugated horseradish peroxidase antibody at room temperature for 1 hour. Staining was visualized with diaminobenzidine, and samples were counterstained with hematoxylin. The details of the protocol have been described.[32]

Stained slides were scanned using a whole slide scanning microscope (Aperio Scanscope CS, Leica Biosystems). A pathologist who was blinded as to the patients' characteristics evaluated every tissue section independently.

Lipid droplet staining

AML12 cells or cryosections (4 μm thick) were washed briefly with PBS for 3 times, followed by incubation with BODIPY (1:250) in PBS for 30 minutes at room temperature. After washing with PBS twice, the cells or sections were fixed with 4% paraformaldehyde, stained with phalloidin plus DRAQ5, and analyzed by confocal microscopy as described above.

Time-of-flight mass cytometry

Time-of-flight mass cytometry was performed for analysis of the expression of the 26 related proteins in atRA-

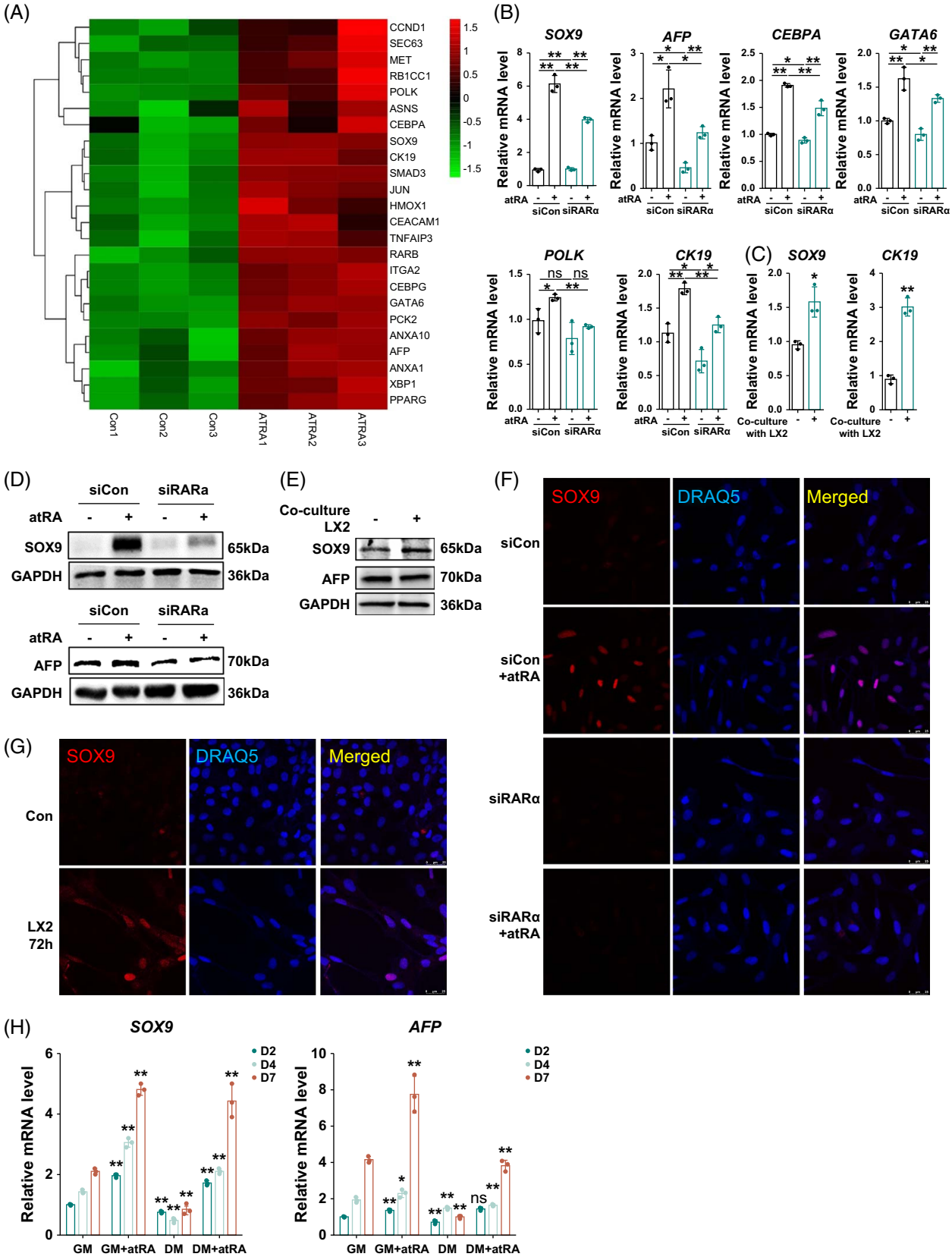

FIGURE 4 Retinoid acid enhanced the stemness of the LPCs. (A) Heatmap showing the upregulated genes involved in stemness maintenance. (B) Relative mRNA levels of SOX9, AFP, CEBPA, GATA6, POLK, and CK19 in HepaRG cells treated with/without atRA, followed by transfection of control or RARα siRNA. (C) Relative mRNA levels of SOX9 and CK19 in HepaRG cells cocultured with/without LX-2 cells for 72 hours. (D) Protein levels of SOX9 and AFP were determined by western blotting in HepaRG cells treated with/without atRA, followed by

transfection of control or RARα siRNA. (E) Protein levels of SOX9 and AFP were determined by western blotting in HepaRG cells cocultured with/without LX-2 cells for 72 hours. (F) Location of SOX9 was detected by immunofluorescence staining in HepaRG cells treated with/without atRA, followed by transfection of control or RARα siRNA. (G) Location of SOX9 was detected by immunofluorescence staining in HepaRG cells cocultured with/without LX-2 for 72 hours. (H) Relative mRNA levels of SOX9 and AFP in HepaRG cells cultured in GM or DM incubated with/without atRA for 2, 4, and 7 days. For qrtPCR, human PPIA was used as the endogenous control. Bars represent mean ± SD. *$p < 0.05$; **$p < 0.01$. For western blotting, GAPDH was used as the loading control. For IF, DRAQ5 was used to stain the nuclei. Scale bars, 25 μm. Images were chosen representatively from 3 independent experiments. Abbreviations: atRA, all-*trans* retinoid acid; DM, differentiation medium; GM, growth medium; IF, immunofluorescence; LPC, liver progenitor cell.

treated HepaRG cells as described.[33] Briefly, HepaRG cells were harvested and labeled with cisplatin to distinguish the dead cells. Then, the cells were stained with an antibody cocktail against target markers and DNA intercalator. Finally, HepaRG cells were detected on the Helios mass cytometer. Based on normalized protein expression of 20 markers (Figure 7B, Supplemental Figure S1, http://links.lww.com/HC9/A950), t-distributed stochastic neighbor embedding (t-SNE) algorithm methods were used to analyze the collected data after normalization using Cytobank (https://www.cytob.ank.org/).

Statistical analysis

Statistical analyses were performed with GraphPad Prism version 6.0 software. The 2-tailed Student *t* test was used to compare 2 independent groups. One-way ANOVA was adopted to test the statistical differences between the means of 2 groups. Variables were described as means and sodium dodecyl sulfate. Statistical significance was indicated as follows: *$p < 0.05$; **$p < 0.01$.

RESULTS

Retinoic acid secreted by activated HSCs induces RARα nuclear translocation in HepaRG LPCs

In ALF, HSCs are activated and secrete high levels of RA into the liver's microenvironment, thereby affecting LPCs. To investigate RA secretion by activated HSCs and its effect on LPCs, freshly isolated phHSCs and immortalized LX-2 HSCs underwent culture for 96 hours or 72 hours, respectively. This facilitated the assessment of RA concentrations and the expression of HSC activation markers. Notably, activated phHSCs and LX-2 cells showed a high level of RA secretion during culture, as evidenced by absorbance measurements at 470 nm of conditioned cell culture supernatant (Figure 1A). Concurrently, there was an upregulation of HSC activation marker expression at the mRNA level, including *α-SMA*, *COL1α1*, *MMP2*, and *MMP9* (Figures 1B, C). Next, immunofluorescence (IF) staining of HepaRG cocultured with LX-2 cells for 72 hours revealed that RARα translocated into the nuclei of HepaRG cells due to LX-2-secreted RA (Figure 1D). Further, treatment with atRA also induced RARα nuclear translocation in HepaRG cells (Figure 1E).

These data show that the RARα pathway in LPC is activated by HSC-secreted RA.

Retinoic acid treatment significantly altered gene expression in HepaRG cells

To analyze the effect of RA on LPC, RNAseq was performed to analyze the transcriptomes of HepaRG cells treated with either DMSO or atRA (n = 3). Genes significantly affected by atRA treatment are shown in the heatmap (Figure 2A). Gene ontology enrichment, enrichment score, and Kyoto Encyclopedia of Genes and Genomes enrichment analysis showed that, in response to atRA treatment in HepaRG cells, the top-upregulated genes were prominently involved in, among others, cytokine-cytokine interaction, PI3K-AKT signaling, ECM-receptor interaction, and pathways related to cancer (Figures 2B–D), while the most downregulated genes were related to metabolism, IL17 signaling, insulin signaling, and cytokine-cytokine interaction (Figures 2E–G). To explore the effect of RA on LPCs in the context of ALF, we focused on pathways crucial for LPC activation, including WNT, Hippo/YAP, stemness, metabolism, and cell survival–related signaling.

Retinoic acid activates WNT signaling in HepaRG cells

According to RNAseq data, the expression of activators and components associated with the WNT signaling pathway exhibited a significant upregulation upon atRA treatment (Figure 3A). To validate the activation of WNT signaling, HepaRG cells were incubated with or without atRA for 24 hours following transfection with RARα siRNA or control siRNA. RARα knockdown efficiency was confirmed by qrt PCR and immunoblotting (Figure 3B). Consistent with RNAseq data, WNT signaling ligands WNT2b and WNT7B were induced by atRA treatment or coculture with LX-2 cells (Figures 3C, D). In addition, atRA-induced WNT2B/7B expression was blunted by RARα knockdown (Figures 3C, D). Both active β-Catenin and total β-Catenin, the

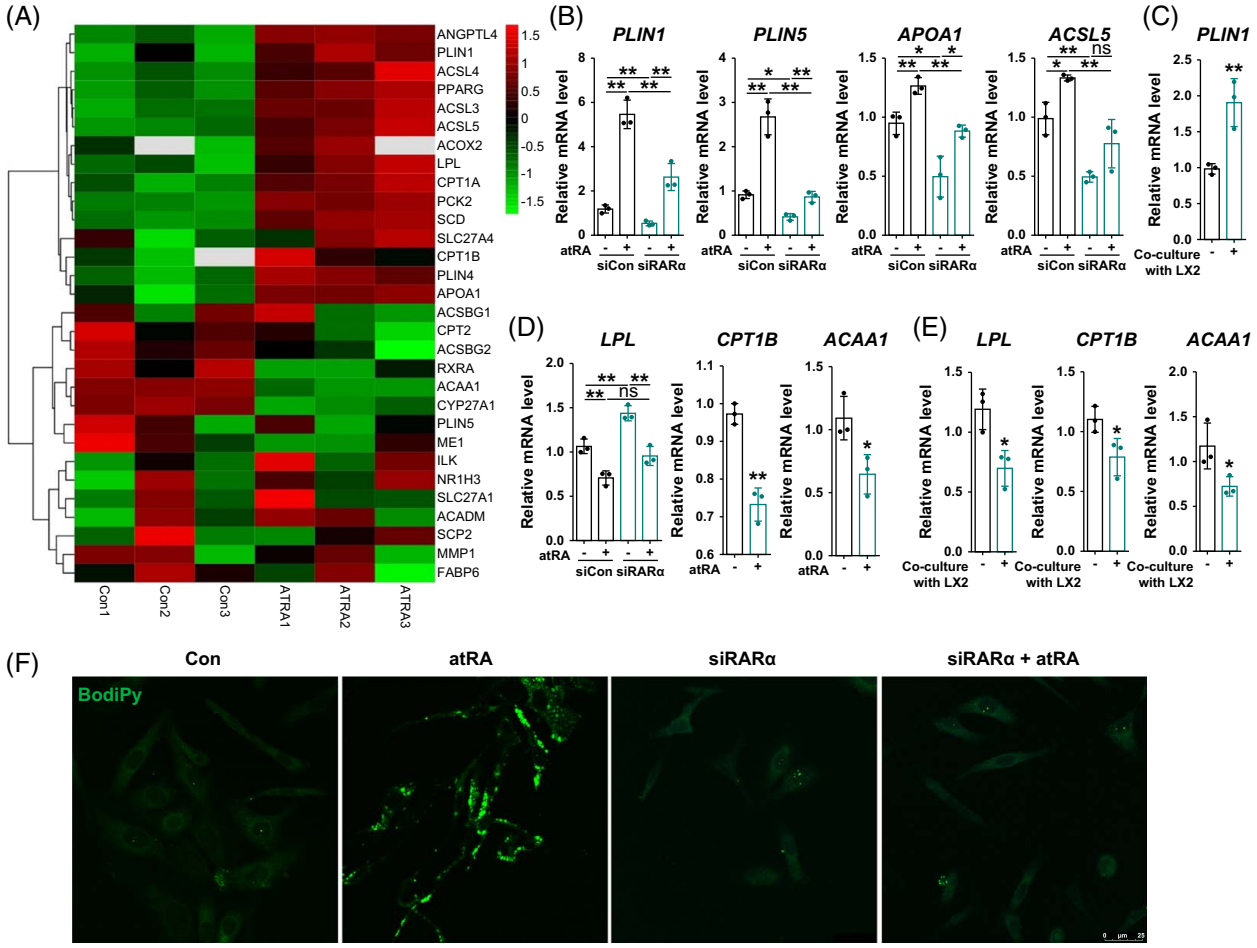

FIGURE 5 RA promotes energy storage in the LPCs. (A) Heatmap showing the downregulated and upregulated genes involved in metabolism upon atRA treatment in HepaRG cells. (B) Relative mRNA levels of PLIN1, PLIN5, APOA1, and ACSL5 in HepaRG cells treated with/without atRA followed by transfection of control or RARα siRNA. (C) Relative mRNA levels of PLIN1 in HepaRG cells cocultured with/without LX-2 cells for 72 hours. (D) Relative mRNA levels of LPL, CPT1B, and ACAA1 in HepaRG cells treated with/without atRA followed by transfection of control or RARα siRNA. (E) Relative mRNA levels of LPL, CPT1B, and ACAA1 in HepaRG cells cocultured with/without LX-2 cells for 72 hours. (F) Lipid droplet accumulation in HepaRG cells treated with/without siRARα and atRA was examined by BodiPy staining. DRAQ5 was used for the nuclear staining. For qrtPCR, human PPIA was used as the endogenous control. Bars represent mean ± SD. *$p < 0.05$; **$p < 0.01$. For BODIPY staining, scale bars, 25 μm. Images were chosen representatively from 3 independent experiments. Abbreviations: atRA, all-*trans* retinoid acid; LPC, liver progenitor cell; RA, retinoic acid.

core components of the WNT signaling pathway, were increased in response to atRA treatment for 4, 8, and 24 hours in HepaRG cells (Figure 3E), which was contingent on RARα expression (Figure 3F). Coculture with LX2 cells for 72 hours similarly enhanced the expression of active and total β-Catenin (Figure 3G). The elevation of active β-Catenin in the nuclear protein fraction of HepaRG cells was further corroborated through immunoblotting analysis following the aforementioned treatments (Figures 3H–J). IF staining of active β-Catenin showed its nuclear translocation, stimulated by atRA in HepaRG cells and disrupted by RARα knockdown (Figure 3K). In contrast, total β-Catenin, typically localized at the cell membrane due to its role in cell-cell adhesion, showed some translocation into the nucleus following atRA treatment or coculture with LX-2 cells (Figures 3L, M). In summary, these findings collectively indicate the activation of the WNT/β-Catenin pathway in HepaRG cells by atRA.

Retinoic acid enhanced the stemness of LPCs

Based on RNAseq, the expression levels of transcription factors associated with stemness were considerably increased following atRA treatment, including *SOX9 alpha fetoprotein* (*AFP*), *CCAAT enhancer binding protein alpha* (*CEBPA*), *CCAAT enhancer binding protein gamma* (*CEBPG*), *GATA binding protein 6* (*GATA6*), *DNA polymerase kappa* (*POLK*), and *keratin 19* (*CK19*) (Figure 4A).

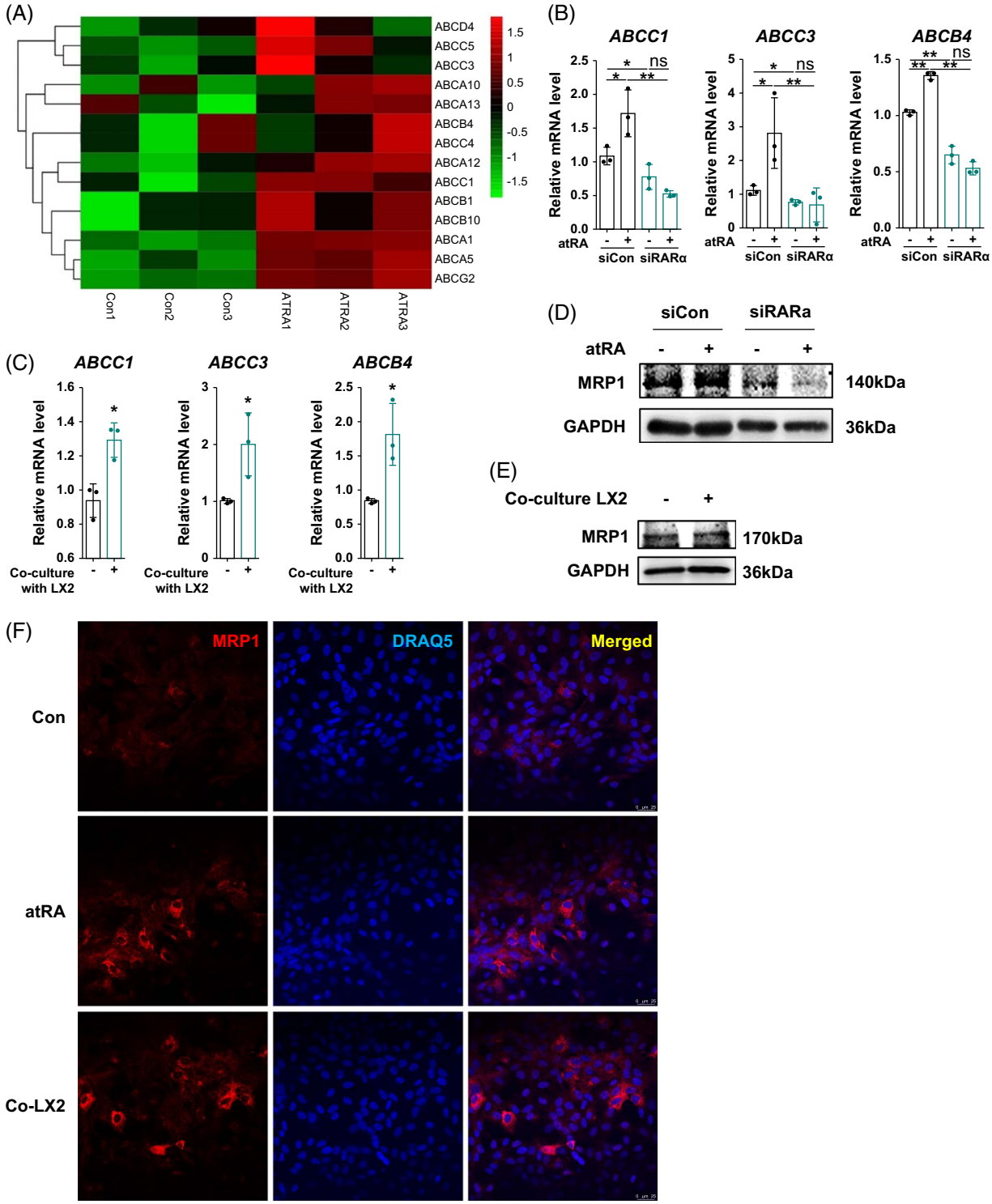

FIGURE 6 RA increases ABC protein expression in HepaRG cells. (A) Heatmap showing the upregulated ABC subfamily genes expression upon atRA treatment in HepaRG cells. (B) Relative mRNA levels of ABCC1, ABCC3, and ABCB4 in HepaRG cells treated with/without atRA followed by transfection of control or RARα siRNA. (C) Relative mRNA levels of ABCC1, ABCC3, and ABCB4 in HepaRG cells cocultured with/without LX2 cells for 72 hours. (D) Protein level of MRP1 was determined by western blotting in HepaRG cells treated with/without atRA followed by transfection of control or RARα siRNA. (E) Protein level of MRP1 was determined by western blotting in HepaRG cells cocultured with/without LX-2 cells for 72 hours. (F) Cellular location of MRP1 was detected by immunofluorescence staining in HepaRG cells treated with/without atRA or coculture with LX-2 cells for 72 hours. For qrtPCR, human PPIA was used as the endogenous control. Bars represent mean ± SD. *$p < 0.05$; **$p < 0.01$. For western blotting, GAPDH was used as the loading control. For IF, DRAQ5 was used to stain the nuclei. Scale bars, 25 μm. Images were chosen representatively from 3 independent experiments. Abbreviations: ABC, ATP-binding cassette; atRA, all-*trans* retinoid acid; IF, immunofluorescence; RA, retinoic acid.

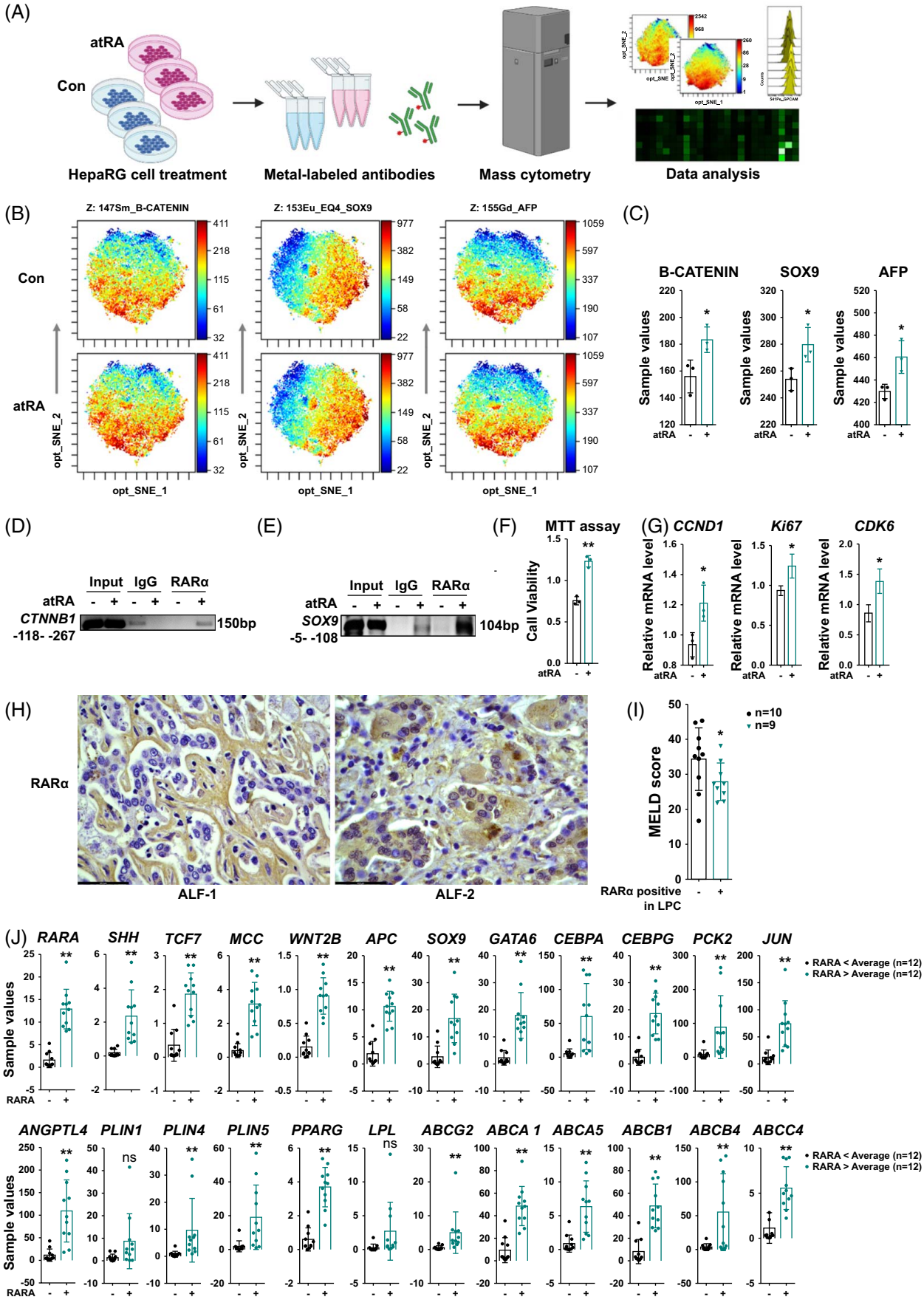
(A)
atRA
Con
HepaRG cell treatment
Metal-labeled antibodies
Mass cytometry
Data analysis
(B)
Z: 147Sm_B-CATENIN
Z: 153Eu_EQ4_SOX9
Z: 155Gd_AFP
Con
atRA
opt_SNE_2
opt_SNE_1
(C)
B-CATENIN
SOX9
AFP
Sample values
atRA
(D)
Input IgG RARα
CTNNB1
-118- -267
150bp
(E)
SOX9
-5- -108
104bp
(F)
MTT assay
Cell Viability
(G)
CCND1
Ki67
CDK6
Relative mRNA level
(H)
RARα
ALF-1
ALF-2
(I)
MELD score
n=10
n=9
RARα positive in LPC
(J)
RARA
SHH
TCF7
MCC
WNT2B
APC
SOX9
GATA6
CEBPA
CEBPG
PCK2
JUN
ANGPTL4
PLIN1
PLIN4
PLIN5
PPARG
LPL
ABCG2
ABCA 1
ABCA5
ABCB1
ABCB4
ABCC4
RARA < Average (n=12)
RARA > Average (n=12)
ns

FIGURE 7 Patients with ALF with positive nuclear RARα in LPCs have a better prognosis. (A) CyTOF analysis of atRA effects on HepaRG cells (created with BioRender.com). (B, C) t-SNE heatmap and sample values of protein expression among the control and atRA treatment groups. (D, E) ChIP assay of RARα binding to the CTNNB1 and SOX9 gene promoter in HepaRG cells upon control or atRA treatment with the PCR amplified products were shown on a 2% agarose gel. Fragment "−118 bp to −267 bp" or "−5 bp to −108 bp" was relative to the transcription start site of CTNNB1 or SOX9 gene, respectively. Rabbit IgG-bound chromatin served as a negative control. (F) MTT assay of HepaRG cells with control or atRA incubation for 72 hours. (G) Relative mRNA levels of CCND1, Ki67, and CDK6 in HepaRG cells treated with/without atRA. (H) IHC staining of RARα in the liver tissue of 21 patients with ALF. (I) MELD score of all patients with ALF with or without RARα nuclear expression. (J) mRNA expression of RARA and the target genes in liver tissue of 24 patients with ALF, extracted from Gene Expression Omnibus DataSets GSE164397. Bars represent mean ± SD. *$p < 0.05$; **$p < 0.01$. Scale bars, 43.5 μm. Images were chosen representatively from IHC staining. Abbreviations: ALF, acute liver failure; atRA, all-*trans* retinoid acid; IHC, immunohistochemistry; LPC, liver progenitor cell; MTT, thiazolyl blue tetrazolium bromide; t-SNE, t-distributed stochastic neighbor embedding.

Among these transcription factors, *SOX9*, *AFP*, *CEBPA*, *GATA6*, *POLK*, and *CK19* mRNA were increased in HepaRG cells following incubation with atRA as verified by qrtPCR. This effect was sustained with RARα expression (Figure 4B). Coculture with LX-2 cells also promoted *SOX9* and *CK19* expression on the mRNA level (Figure 4C). Western blotting substantiated the stimulatory impact of atRA on SOX9 and AFP protein expression, which was attenuated by RARα knockdown (Figure 4D). Coculture with LX-2 cells also increased SOX9 expression in HepaRG cells, although AFP expression was not increased (Figure 4E). IF staining showed a positive nuclear signal for SOX9 in HepaRG cells treated with either atRA (Figure 4F) or cocultured with LX-2 cells (Figure 4G). The atRA-induced SOX9 nuclear expression was impeded by transfection with RARα siRNA (Figure 4F). Given the crucial role of SOX9 in regulating the transition between hepatic and biliary cell phenotypes during both liver development and regeneration, and AFP being a well-known marker for LPC,[34,35] we investigated SOX9 and AFP mRNA expressions in HepaRG cells cultured in a growth medium or differentiation (LPC-to-hepatocyte differentiation) medium treated with atRA on days 2, 4, and 7. Growth medium alone promoted SOX9 and AFP mRNA expression, with atRA further enhancing this effect as opposed to differentiation (LPC-to-hepatocyte differentiation) medium. However, atRA incubation rescued differentiation (LPC-to-hepatocyte differentiation) medium-mediated inhibitory outcomes (Figure 4H).

These data suggest that atRA promotes the stemness of HepaRG cells by upregulating the expression of stem cell markers.

Retinoic acid promotes energy storage in the LPCs

The liver is essential to the body's metabolism as it governs energy storage build-up and depletion.[36] Under ALF conditions, when most hepatocytes are damaged or necrotic, LPCs are essential for regulating metabolism. Based on our RNAseq data, atRA demonstrated a dual impact on gene expression, either promoting or inhibiting genes associated with lipogenesis or β-oxidation (Figure 5A). We examined the mRNA expression of genes involved in lipogenesis upon atRA treatment. The qrtPCR data showed that atRA-induced *perilipin 1* (*PLIN1*), *perilipin 5* (*PLIN5*), *apolipoprotein A1* (*APOA1*), and *acyl-CoA synthetase long-chain family member 5* (A*CSL5*) expressions on mRNA level, in a RARα-dependent manner (Figure 5B). Unexpectedly, coculture with LX-2 cells led to only *PLIN1* mRNA expression to increase (Figure 5C). This may be attributed to the secretion of TGF-β by activated HSCs, which, in addition to RA, inhibits lipogenesis, counteracting RA's impact on fatty acid metabolism.[37] Further, we tested the mRNA expression of genes involved in β-oxidation. qrtPCR validated that atRA treatment or coculture with LX-2 inhibited *lipoprotein lipase* (*LPL*), *carnitine palmitoyl transferase 1B* (*CPT1B*), and *acetyl-CoA acyltransferase 1* (*ACAA1*) mRNA expression in HepaRG cells (Figure 5D). Coculture with LX-2 cells also reduced *LPL*, *CPT1B*, and *ACAA1* mRNA expression (Figure 5E). Since CPT1B is the rate-controlling enzyme of the long-chain fatty acid β-oxidation pathway and ACAA1 is an enzyme involved in peroxisomal β-oxidation, these results implicate that atRA diminished β-oxidation in HepaRG cells. Notably, atRA incubation caused lipid droplet accumulation in HepaRG cells and relied on RARα expression as well (Figure 5F), although the inhibition of CPT1B and ACAA1 by atRA was independent of RARα (Figure 5D).

These results illustrate that atRA exerts a dual effect on genes related to fatty acid β-oxidation and lipogenesis, promoting energy storage in HepaRG cells. In the presence of activated HSCs, TGF- mitigates atRA's impact on fatty acid metabolism.

Retinoid acid increases ABC transporters expression in HepaRG cells

Several members of the ATP-binding cassette (ABC) transporter superfamily exhibited upregulation in response to atRA treatment in HepaRG cells, including, among others, *ABCG2*, *ABCA5*, *ABCA1*, *ABCC3*, and *ABCB4* (Figure 6A). Verified by qrtPCR, atRA significantly induced the mRNA expression of *ABCC1*, *ABCC3*, and *ABCB4* in an RARα-dependent manner (Figure 6B), which was further demonstrated by coculture with LX-2 cells for 72 hours (Figure 6C). Immunoblotting showed increased expression of

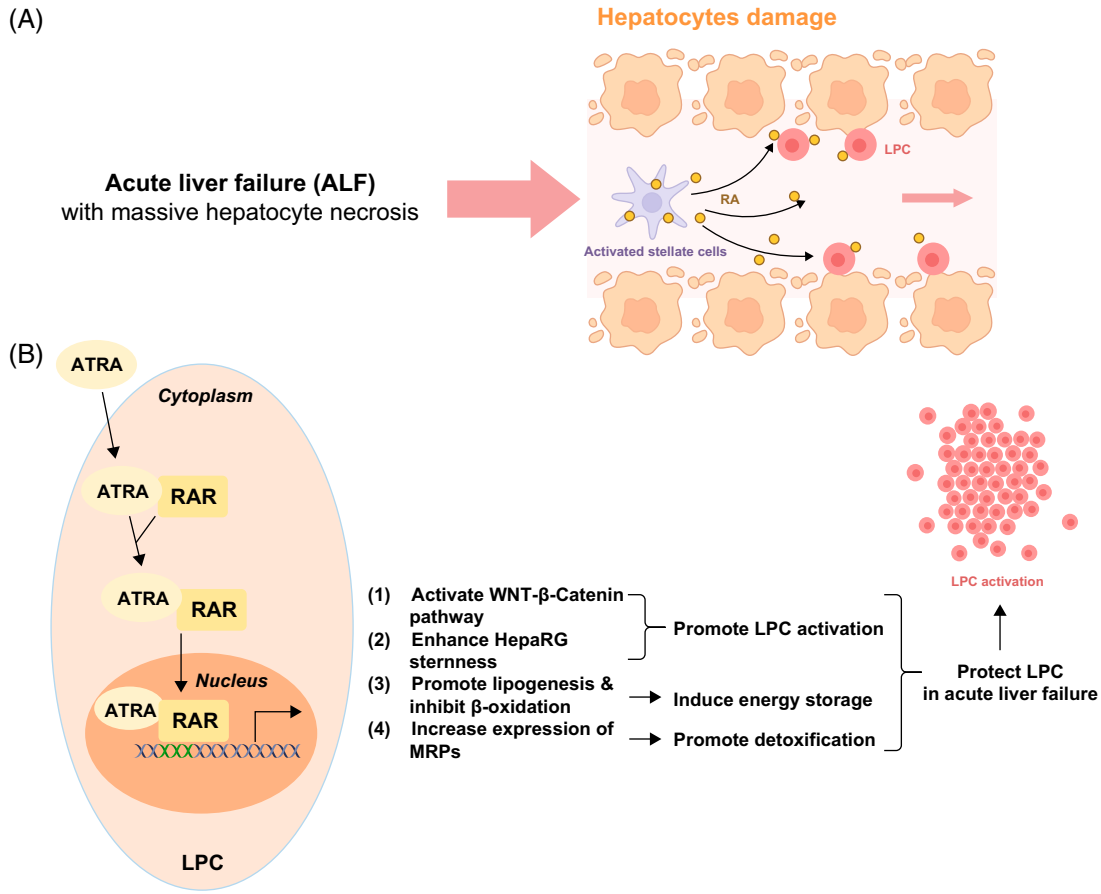

FIGURE 8 Schematic diagram of RA's role in regulating LPC activation under ALF conditions. (A) In ALF, activated HSCs secrete high amounts of RA. Since most of the hepatocytes are damaged or deceased, LPCs are the main cells capable of conveying RA signaling. (B) RA translocates with RARα into the nuclei in LPCs to induce the transcription of retinoid-responsive genes, including members of the WNT/β-Catenin pathway, regulating cellular stemness, metabolic regulation, and multidrug resistance to enhance the stemness, energy storage, and detoxification in LPCs, thus enabling the LPCs to survive and drive liver regeneration under ALF conditions (created with BioRender.com). Abbreviations: ALF, acute liver failure; LPC, liver progenitor cell; RA, retinoic acid.

ABCC1/MRP1 on protein level upon atRA stimulation, which was blocked by siRARα (Figure 6D). Coculture with LX-2 cells also increased MRP1 protein expression compared to control HepaRG cells (Figure 6E). In addition, IF staining showed increased membrane-bound expression of MRP1 in HepaRG cells triggered by atRA-RARα signaling (Figure 6F).

Proteins encoded by the ABC family play an important role in the transport of biliary compounds, particularly for the intestinal excretion of organic anions, and are implicated in multidrug resistance. Upregulation of these genes by atRA suggests a potential role in creating a permissive niche for the survival of LPCs under ALF conditions.

Patients with ALF with positive nuclear RARα in LPCs have a better prognosis

To corroborate our findings derived from mRNA sequencing analysis, we performed a single-cell CyTOF analysis. The schematic workflow is delineated in Figure 7A. The CyTOF-generated data set underwent identification of individual cells for visualization by single-cell proteomic analysis using the t-SNE algorithm. The resulting t-SNE heatmap was portrayed as a bi-axial scatter plot with one plot representing a single cell. Each dot's position on the plot was determined by the combined expression of all proteins within that specific cell. The t-SNE heatmap of β-Catenin, SOX9, and AFP indicated that while there was no significant difference in the protein expression patterns between the 2 groups of cells, the red dots denoting higher expression levels were found mostly in atRA-treated HepaRG cells (Figure 7B). The corresponding protein expression values for each sample were also depicted in the histograms (Figure 7C). To gain deeper insights into the mechanism underlying atRA/RARα-induced upregulation of SOX9 and AFP, a chromatin immunoprecipitation (ChIP) assay was performed. The results revealed a significant induction of RARα binding to the *CTNNB1* gene promoter (−118 to −267) with its predicted binding site being AGGCCGCGCAGCGGGCA and *SOX9* (−5 to −108) with its predicted binding site being GGGTGGCTCTAAGGTGA following incubation with atRA (Figures 7D, E). Given the indications from

our findings that atRA promoted LPC activation, characterized by increased cell proliferation, we conducted an MTT assay. The results demonstrate that incubation with atRA for 72 hours significantly enhances HepaRG cell viability (Figure 7F), potentially through the upregulation of *CCND1*, *Ki67*, and *CDK6* (Figure 7G).

Next, we performed immunohistochemistry staining of RARα in the liver tissue of patients with ALF. Nineteen patients with ALF were categorized into 2 cohorts based on positive or negative RARα nuclear staining in LPCs. Ten patients showed negative RARα nuclear staining while 9 patients stained positive (Figure 7H). To correlate these findings with disease severity, the MELD score was calculated for each patient. Notably, patients with ALF maintaining nuclear RARα expression had a lower MELD score (Figure 7I), suggesting a potential correlation between RARα signaling and a favorable prognosis in ALF. To further validate the association between RARα activation and the identified signaling pathways (Figures 3–6) in patients with ALF, we extracted the relevant genes from the Gene Expression Omnibus data set (GSE164397) that comprises mRNA expression data from liver tissue of pediatric patients with ALF. The 24 patients with ALF were divided into *RARA*− (n = 12) or *RARA*+ (n = 12) groups according to the expression value of *RARA* being above or below its average. In patients in the *RARA*+ group with ALF, there was a significant upregulation of WNT signaling (*SHH*, *TCF7*, *MCC*, *WNT2B*, and *APC*), stemness markers (*SOX9*, *GATA6*, *CEBPA*, *CEBPG*, *PCK2*, and *JUN*), lipogenesis (*ANGPTL4*, *PLIN1*, *PLIN4*, *PLIN5*, and PPARG), and ABC transporters (*ABCG2*, *ABCA1*, *ABCA5*, *ABCB1*, *ABCB4*, and *ABCC4*) (Figure 7J), corroborating our observations in HepaRG cells.

DISCUSSION

The liver shows a remarkable regenerative capacity under the most adverse conditions. Its ability to do so is primarily due to 2 main mechanisms: hepatocyte-mediated and/or LPC-mediated regeneration.[38] The predominant mode of regeneration is driven by already differentiated hepatocytes undergoing proliferation, while the second mode requires the differentiation of hepatic stem cells (LPCs) into hepatocytes. The latter becomes particularly crucial when the number of damaged hepatocytes exceeds a certain threshold, such as in the context of ALF.[4,38] The initiation of LPC-mediated regeneration necessitates LPC activation, histologically manifested as ductular reaction.[4] To date, the signals within the microenvironment of ALF livers that instigate LPC activation and the subsequent regeneration process remain largely elusive. This study has unveiled that RA/RARα signaling may be responsible for LPC activation by augmenting their stemness, enhancing energy storage, and increasing drug resistance (Figure 8), all of which are significant for subsequent liver regeneration and correlate with a better prognosis for patients with ALF.

To investigate the stemness of HepaRG cells treated with atRA, we analyzed RNAseq data and verified them by qrtPCR, revealing a significant upregulation of WNT signaling and LPC makers, including SOX9, AFP, and CK7. The WNT/β-Catenin pathway is a highly conserved and tightly controlled molecular mechanism that regulates hepatobiliary development and cell fate during embryogenesis, as well as liver homeostasis and repair in adulthood.[39] Besides, WNT signaling is essential during liver regeneration as it is key for the activation of LPCs, which are LPCs.[40] In addition, WNT seems to play a role in LPC expansion and differentiation.[41] However, aberrant activation of the WNT/β-Catenin pathway entails a high risk of HCC development,[42] indicating the need to precisely target atRA/RAR signaling at specific stages during ALF. It becomes crucial to target the initiation stage of ALF when LPCs need activation rather than a later stage when LPCs differentiate into hepatocytes, as the latter potentially promote HCC development. One recent study found that atRA acts as a regulator of the lineage plasticity of mouse hair follicle stem cells by inducing SOX9 promoter activity and modulating their response to WNT and BMP (bone morphogenetic protein) signals.[43] However, the underlying mechanisms of atRA in regulating SOX9 and WNT signaling are not fully understood. According to our results (Figures 7D, E), it appears that atRA-activated RARα can bind to the gene promoters of *CTNNB1* and *SOX9*, thus inducing their expression. Whether there is a priority or crosstalk between SOX9 and WNT/β-Catenin mediated by RA warrants further investigation. Studies found that as β-Catenin lacks the intrinsic ability to bind to DNA, its interaction with target genes relies on the recruitment of coactivators and other transcription factors, such as hypoxia-inducible factor 1α (HIF1α),[44] forkhead box protein O (FOXO),[45] and SOX family transcription factors.[46] Combining these findings with our own results, we propose that atRA/RARα may activate WNT/β-Catenin signaling and induce SOX9 upregulation, cooperating to increase LPC marker expression, for example, AFP. This is supported by our observation that knockdown of SOX9 abolished atRA-induced AFP expression both on mRNA and protein levels (Supplemental Figure S2, http://links.lww.com/HC9/A950), suggesting that atRA promotes AFP expression possibly SOX9-dependently.

The liver is an important metabolic organ and plays an essential role in the body's energy metabolism.[36] Ensuring a sufficient energy supply for glucose-dependent organs and cells, such as the brain, heart, and LPCs in the liver, is imperative for the body's resilience to systemic illnesses like ALF.[47] Therefore, we investigated the regulatory impact of atRA on metabolic processes in HepaRG cells. Our findings demonstrated that atRA inhibits fatty acid β-

oxidation while promoting lipogenesis in LPCs, opposing its function in hepatocytes,[14] and we postulate that this regulation results in enhanced energy storage, a critical factor for the survival of LPCs under ALF conditions. Nonetheless, the intricate mechanisms underlying these regulatory actions warrant further exploration. In addition, we observed a significant induction of ABC-family transporters by atRA. Apart from their role in cholesterol and bile acid transport, they also participate in detoxification and multidrug resistance, thus further protecting LPCs from damage.[48] While studies have identified the regulation of ABCC2, ABCC3, ABCC4, and ABCB11 by atRA-RAR/RXR in hepatocytes,[49,50] there is a paucity of research in LPCs. Based on our analyses, ABC transporters can be upregulated by atRA in LPCs, partially depending on RARα, with the underlying mechanisms again warranting further investigation.

In our study, we observed that patients with ALF maintaining nuclear expression of RARα in LPCs exhibited better MELD scores, indicative of improved survival. However, to further validate our findings, more analyses should encompass additional clinical outcomes from our patient cohort. Evaluating parameters such as the likelihood of sepsis, ascites, bacterial infections, renal failure, and encephalopathy during ALF would provide a comprehensive understanding of the clinical implications. In conclusion, our investigation assessed the effects of RA secreted by activated HSCs on LPCs and implies that the RA-RAR pathway could potentially serve as a target to activate LPCs, especially at the early stage of ALF, thereby promoting liver regeneration, which holds promise for developing improved treatment options for individuals suffering from ALF.

AUTHOR CONTRIBUTIONS

Conception, design, and hypothesis: Shan-Shan Wang. In vitro experiments: Sai Wang, Frederik Link, Stefan Munker, Shan-Shan Wang, Wenjing Wang, Rilu Feng, Yujia Li, and Ye Yao. Patients sampling and pathological experiments: Sai Wang, Frederik Link, Hui Liu, Chen Shao, Huiguo Ding, and Hong-Lei Weng. Bioinformatics analysis: Sai Wang, Frederik Link, and Shan-Shan Wang. Drafting the article: Sai Wang, Frederik Link, and Shan-Shan Wang. Data discussion, reviewing, and editing the article critically: Sai Wang, Frederik Link, Shan-Shan Wang, Roman Liebe, Honglei Weng, Steven Dooley, Huiguo Ding, and Matthias P.A. Ebert.

ACKNOWLEDGMENTS

The authors acknowledge the support of the LIMa Live Cell Imaging at Microscopy Core Facility Platform Mannheim (CFPM).

FUNDING INFORMATION

The study was supported by the Chinese-German Cooperation Group projects GZ1263 (Steven Dooley), M-0099 (Steven Dooley), and M-0200 (Shan-Shan and Wang); Beijing Municipal Natural Science Foundation (7212052 to Shan-Shan Wang); Deutsche Forschungsgemeinschaft WE 5009/9-1 (Hong-Lei Weng); Beijing Municipal Public Welfare Development and Reform Pilot Project for Medical Research Institutes (PWD&RPP-MRI, JYY2021-10); and Federal Ministry of Education and Research (BMBF) Programs (Liver Systems Medicine [LiSyM], grant number PTJ-031L0043 and LiSyM-HCC, grant number PTJ-031L0257A).

CONFLICTS OF INTEREST

The authors have no conflicts to report.

ORCID

Sai Wang https://orcid.org/0000–0002–9731–3948
Frederik Link https://orcid.org/0000–0002–8384–705X
Roman Liebe https://orcid.org/0000–0002–3199–5595
Ye Yao https://orcid.org/0000–0001–6642–4226
Hui Liu https://orcid.org/0000–0001–8212–5285
Matthias P.A. Ebert https://orcid.org/0000–0003–3228–5138
Huiguo Ding https://orcid.org/0000–0002–8716–4926
Steven Dooley https://orcid.org/0000–0002–4840–6240
Hong-Lei Weng https://orcid.org/0000–0003–1414–303X

REFERENCES

1. Lefkowitch JH. The pathology of acute liver failure. Adv Anat Pathol. 2016;23:144–58.
2. Hall JE. Guyton and Hall Textbook of Medical Physiology, 12th ed. Saunders; 2011.
3. Lucke B, Mallory T. The fulminant form of epidemic hepatitis. Am J Pathol. 1946;22:867–947.
4. Weng HL, Cai X, Yuan X, Liebe R, Dooley S, Li H, et al. Two sides of one coin: Massive hepatic necrosis and progenitor cell-mediated regeneration in acute liver failure. Front Physiol. 2015;6:178.
5. Roskams TA, Theise ND, Balabaud C, Bhagat G, Bhathal PS, Bioulac-Sage P, et al. Nomenclature of the finer branches of the biliary tree: Canals, ductules, and ductular reactions in human livers. Hepatology. 2004;39:1739–45.
6. Geerts A. History, heterogeneity, developmental biology, and functions of quiescent hepatic stellate cells. Semin Liver Dis. 2001;21:311–35.
7. Ghyselinck NB, Duester G. Retinoic acid signaling pathways. Development. 2019;146. doi:10.1242/dev.167502
8. Wake K, Sato T. Intralobular heterogeneity of perisinusoidal stellate cells in porcine liver. Cell Tissue Res. 1993;273:227–37.
9. Friedman SL. Hepatic stellate cells: Protean, multifunctional, and enigmatic cells of the liver. Physiol Rev. 2008;88:125–72.
10. Li Y, Fan W, Link F, Wang S, Dooley S. Transforming growth factor beta latency: A mechanism of cytokine storage and signalling regulation in liver homeostasis and disease. JHEP Rep. 2022;4:100397.
11. D'Ambrosio DN, Walewski JL, Clugston RD, Berk PD, Rippe RA, Blaner WS. Distinct populations of hepatic stellate cells in the mouse liver have different capacities for retinoid and lipid storage. PLoS One. 2011;6:e24993.
12. Li B, Cai SY, Boyer JL. The role of the retinoid receptor, RAR/RXR heterodimer, in liver physiology. Biochim Biophys Acta Mol Basis Dis. 2021;1867:166085.

13. Idres N, Marill J, Flexor MA, Chabot GG. Activation of retinoic acid receptor-dependent transcription by all-trans-retinoic acid metabolites and isomers. J Biol Chem. 2002;277:31491–8.
14. Berry DC, DeSantis D, Soltanian H, Croniger CM, Noy N. Retinoic acid upregulates preadipocyte genes to block adipogenesis and suppress diet-induced obesity. Diabetes. 2012;61:1112–21.
15. Tsuchiya H, Ikeda Y, Ebata Y, Kojima C, Katsuma R, Tsuruyama T, et al. Retinoids ameliorate insulin resistance in a leptin-dependent manner in mice. Hepatology. 2012;56:1319–30.
16. Cortes E, Lachowski D, Rice A, Chronopoulos A, Robinson B, Thorpe S, et al. Retinoic acid receptor-beta is downregulated in hepatocellular carcinoma and cirrhosis and its expression inhibits myosin-driven activation and durotaxis in hepatic stellate cells. Hepatology. 2019;69:785–802.
17. Cai SY, Mennone A, Soroka CJ, Boyer JL. All-trans-retinoic acid improves cholestasis in alpha-naphthylisothiocyanate-treated rats and Mdr2-/- mice. J Pharmacol Exp Ther. 2014;349:94–8.
18. Mezaki Y, Yoshikawa K, Yamaguchi N, Miura M, Imai K, Kato S, et al. Rat hepatic stellate cells acquire retinoid responsiveness after activation in vitro by post-transcriptional regulation of retinoic acid receptor alpha gene expression. Arch Biochem Biophys. 2007;465:370–9.
19. Erkelens MN, Mebius RE. Retinoic acid and immune homeostasis: A balancing act. Trends Immunol. 2017;38:168–80.
20. Cippitelli M, Ye J, Viggiano V, Sica A, Ghosh P, Gulino A, et al. Retinoic acid-induced transcriptional modulation of the human interferon-gamma promoter. J Biol Chem. 1996;271:26783–93.
21. Hoang TX, Jung JH, Kim JY. All-trans retinoic acid enhances bacterial flagellin-stimulated proinflammatory responses in human monocyte THP-1 cells by upregulating CD14. Biomed Res Int. 2019;2019:8059312.
22. Kim CH. Retinoic acid, immunity, and inflammation. Vitam Horm. 2011;86:83–101.
23. Devalaraja S, To TKJ, Folkert IW, Natesan R, Alam MZ, Li M, et al. Tumor-derived retinoic acid regulates intratumoral monocyte differentiation to promote immune suppression. Cell. 2020;180:1098–1114 e1016.
24. Gundra UM, Girgis NM, Gonzalez MA, San Tang M, Van Der Zande HJP, Lin JD, et al. Vitamin A mediates conversion of monocyte-derived macrophages into tissue-resident macrophages during alternative activation. Nat Immunol. 2017;18:642–53.
25. Scott CL, Zheng F, De Baetselier P, Martens L, Saeys Y, De Prijck S, et al. Bone marrow-derived monocytes give rise to self-renewing and fully differentiated Kupffer cells. Nat Commun. 2016;7:10321.
26. Li H, Xia Q, Zeng B, Li ST, Liu H, Li Q, et al. Submassive hepatic necrosis distinguishes HBV-associated acute on chronic liver failure from cirrhotic patients with acute decompensation. J Hepatol. 2015;63:50–9.
27. Wan P, Xu D, Zhang J, Li Q, Zhang M, Chen X, et al. Liver transplantation for biliary atresia: A nationwide investigation from 1996 to 2013 in mainland China. Pediatr Transplant. 2016;20:1051–9.
28. Reiter FP, Ye L, Ofner A, Schiergens TS, Ziesch A, Brandl L, et al. p70 ribosomal protein S6 kinase is a checkpoint of human hepatic stellate cell activation and liver fibrosis in mice. Cell Mol Gastroenterol Hepatol. 2022;13:95–112.
29. Marion MJ, Hantz O, Durantel D. The HepaRG cell line: Biological properties and relevance as a tool for cell biology, drug metabolism, and virology studies. Methods Mol Biol. 2010;640:261–72.
30. Abmayr SM, Yao T, Parmely T, Workman JL. Preparation of nuclear and cytoplasmic extracts from mammalian cells. Curr Protoc Mol Biol. 2006; Chapter 12: Unit 12 11.
31. Wang S, Feng R, Wang SS, Liu H, Shao C, Li Y, et al. FOXA2 prevents hyperbilirubinaemia in acute liver failure by maintaining apical MRP2 expression. Gut. 2023;72:549–59.
32. Weng HL, Liu Y, Chen JL, Huang T, Xu LJ, Godoy P, et al. The etiology of liver damage imparts cytokines transforming growth factor beta1 or interleukin-13 as driving forces in fibrogenesis. Hepatology. 2009;50:230–43.
33. Wang Y, Yan Y, Huo Y, Pang Y, Chan L, Wang S, et al. mRNA sequencing and CyTOF analysis revealed ASPP2 altered the response patterns of hepatocellular carcinoma HepG2 cells to usnic acid. Naunyn Schmiedebergs Arch Pharmacol. 2023;396:1847–56.
34. Furuyama K, Kawaguchi Y, Akiyama H, Horiguchi M, Kodama S, Kuhara T, et al. Continuous cell supply from a Sox9-expressing progenitor zone in adult liver, exocrine pancreas and intestine. Nat Genet. 2011;43:34–41.
35. Kuhlmann WD, Peschke P. Hepatic progenitor cells, stem cells, and AFP expression in models of liver injury. Int J Exp Pathol. 2006;87:343–59.
36. Rui L. Energy metabolism in the liver. Compr Physiol. 2014;4:177–97.
37. Han M, Nwosu ZC, Pioronska W, Ebert MP, Dooley S, Meyer C. Caveolin-1 impacts on TGF-beta regulation of metabolic gene signatures in hepatocytes. Front Physiol. 2019;10:1606.
38. Miyajima A, Tanaka M, Itoh T. Stem/progenitor cells in liver development, homeostasis, regeneration, and reprogramming. Cell Stem Cell. 2014;14:561–74.
39. Clevers H, Nusse R. Wnt/beta-catenin signaling and disease. Cell. 2012;149:1192–205.
40. Nejak-Bowen KN, Monga SP. Beta-catenin signaling, liver regeneration and hepatocellular cancer: sorting the good from the bad. Semin Cancer Biol. 2011;21:44–58.
41. Williams JM, Oh SH, Jorgensen M, Steiger N, Darwiche H, Shupe T, et al. The role of the Wnt family of secreted proteins in rat oval "stem" cell-based liver regeneration: Wnt1 drives differentiation. Am J Pathol. 2010;176:2732–42.
42. Russell JO, Monga SP. Wnt/beta-catenin signaling in liver development, homeostasis, and pathobiology. Annu Rev Pathol. 2018;13:351–78.
43. Tierney MT, Polak L, Yang Y, Abdusselamoglu MD, Baek I, Stewart KS, et al. Vitamin A resolves lineage plasticity to orchestrate stem cell lineage choices. Science. 2024;383:14.
44. Kaidi A, Williams AC, Paraskeva C. Interaction between beta-catenin and HIF-1 promotes cellular adaptation to hypoxia. Nat Cell Biol. 2007;9:210–7.
45. Essers MA, de Vries-Smits LM, Barker N, Polderman PE, Burgering BM, Korswagen HC. Functional interaction between beta-catenin and FOXO in oxidative stress signaling. Science. 2005;308:1181–4.
46. Kormish JD, Sinner D, Zorn AM. Interactions between SOX factors and Wnt/beta-catenin signaling in development and disease. Dev Dyn. 2010;239:56–68.
47. Van Wyngene L, Vandewalle J, Libert C. Reprogramming of basic metabolic pathways in microbial sepsis: therapeutic targets at last? EMBO Mol Med. 2018;10:e8712.
48. Ceballos MP, Rigalli JP, Cere LI, Semeniuk M, Catania VA, Ruiz ML. ABC transporters: Regulation and association with multidrug resistance in hepatocellular carcinoma and colorectal carcinoma. Curr Med Chem. 2019;26:1224–50.
49. Chen W, Cai SY, Xu S, Denson LA, Soroka CJ, Boyer JL. Nuclear receptors RXRalpha:RARalpha are repressors for human MRP3 expression. Am J Physiol Gastrointest Liver Physiol. 2007;292:G1221–7.
50. Kassam A, Miao B, Young PR, Mukherjee R. Retinoid X receptor (RXR) agonist-induced antagonism of farnesoid X receptor (FXR) activity due to absence of coactivator recruitment and decreased DNA binding. J Biol Chem. 2003;278:10028–32.

How to cite this article: Wang S, Link F, Munker S, Wang W, Feng R, Liebe R, et al. Retinoic acid generates a beneficial microenvironment for liver progenitor cell activation in acute liver failure. Hepatol Commun. 2024;8:e0483. https://doi.org/10.1097/HC9.0000000000000483